# Frequency Domain Transient Analysis of Resonant Behavior for Different HV Overhead Line and Underground Cable Configurations

L. Wu, P. A. A. F. Wouters, E. F. Steennis

***Abstract*—Electrical resonant behavior in a power transmission system as a result of switching or other transient generating phenomena will depend on the components applied. These components are part of a transmission system based on overhead lines (OHL) with or without embedded underground cables for the Dutch TSO TenneT. Electromagnetic transient program (EMTP) theory (in time domain) based simulation tools are nowadays widely used to analyze power transmission systems, but become time-consuming for studying effect of different parameters in large scale networks.**

**This paper applies 1) an alternative approach to solve the differential equations composed by the system impedance and admittance matrices; 2) uses Discrete Fourier Transformation (DFT) and ABCD-matrix in frequency domain to analyze the transients. The requirement to use small simulation time-steps to correctly simulate shorter sections inside the network in time domain analysis is omitted. The approach is applied to calculate the resonant transient of a large network (combining OHL with partly 6 and partly 12 phase conductors on a single tower, and Cable with 12 mutually coupled single-core cables) located at the Randstad area in the Netherlands, and to study the influence of different network configurations on the resonant grid behavior, e.g. the influence of cable joints, number of cables, with or without cables, and so on. A comparison between this approach and PSCAD/EMTDC based on a simplified cable configuration shows that both methods give same results.**

***Keywords*: Frequency domain analysis, power system transients, transmission lines.**

## I. Introduction

NEW HV transmission systems often include underground power cables in series with overhead lines (OHL) [1]-[3]. Sometimes two cables are parallel connected to each phase of one circuit to acquire the demand energy transmission capacity, meaning totally 12 mutually coupled cables for a double circuit. This applies for TenneT's cable connection in the "South-ring" of the Randstad area in The Netherlands [4]. The double cable circuit, which is situated between two overhead lines of 4.0 km and 6.0 km, is further divided into 12 minor sections, with per minor section an average length of about 0.9 km. These minor sections are connected via cable joints: either cross-bonding joint or straight through joint. In TenneT's planned "North-ring" of the Randstad area, the cable minor sections will have shorter length and are combined with OHLs in a more complex manner. To study effects of alternatives and the effect of parameter variation an efficient analysis approach is preferred.

Each cable has six parts, conductive core with stranded copper wires, semi-conducting layer, XLPE insulation layer, semi-conducting layer, conductive screen layer, and PE outer sheath layer. The underground cables are buried mainly in two different ways: direct buried and with a horizontal directional drilling (HDD). For resonant transient behavior the distance between each cable pair and the depth of each cable with respect to the soil surface are of main importance. Besides, along the cable connection, the earth resistivity varies according to different earth type and condition. Each parameter described above will have either a strong or a weak impact on the resonant transient behavior (e.g. over-voltage of an unloaded transmission line caused by a switching surge).

EMTP-theory ([5]) based simulation methods, which are nowadays widely used in analyzing resonant transient of power systems, can be inefficient and time-consuming when dealing with a complex configuration like the mixed OHL and cable connections in the "South-ring" mentioned above. Large number of mutually coupled cables increases the difficulty in finding fitting parameters in the curve-fitting process ([5], [6]) for solving differential equations composed by the system impedance and admittance. Short length of each cable minor section (e.g. 0.9 km) requires short simulation time steps (e.g. down to 0.5 μs) so that the total simulation duration is prolonged. This paper applies frequency domain modeling with frequency-dependent parameters to both calculate the resonant transient behavior and to analyze the impact of each parameter on transients.

Section II presents detailed configuration of the mixed OHL and cable transmission line in the "South-ring". In Section III, first, the ABCD-matrix of the transmission line is constructed from the differential equations composed by impedance and admittance matrices (without curve fitting method). Next, the ABCD-matrix together with Discrete Fourier Transformation (DFT) techniques are used to analyze

This work was financially supported by TenneT TSO B.V. within the framework of the Randstad380 cable research project, Arnhem, the Netherlands.

L. Wu, P.A.A.F. Wouters, and E.F. Steennis are with the Electrical Energy Systems group, Department of Electrical Engineering, Eindhoven University of Technology, P.O.Box 513, 5600 MB Eindhoven, the Netherlands (e-mail: lei.wu@tue.nl).

E.F. Steennis is also with DNV KEMA Energy & Sustainability, P.O.Box 9035, 6800 ET, Arnhem, the Netherlands.

Paper submitted to the International Conference on Power Systems Transients (IPST2013) in Vancouver, Canada July 18-20, 2013.

the over-voltage caused by any disturbance, which can be represented by an equivalent source, in no-load condition (without simulation time steps). In Section IV, the disturbance is assumed to be the standard switching surge waveform, and the frequency range of the response is calculated up to 10 kHz, sufficient to analyze resonant effects in the circuit. The considered circuit alternatives are: different radii of the conductive core of each cable, earth resistivity, trench types, phase sequences, lengths of cable minor section, number of cable major sections, number of cables, sequences of combined OHL and cable; with and without cable, with and without cable joints.

## II. Reference Configuration

The general configuration of the combined OHL and cable system is shown in Fig. 1. Here, for clearness, only the 380 kV level connections are shown. Detailed drawings are presented in the following subsections. This configuration will be the reference for the analysis based on different parameters in Section IV.

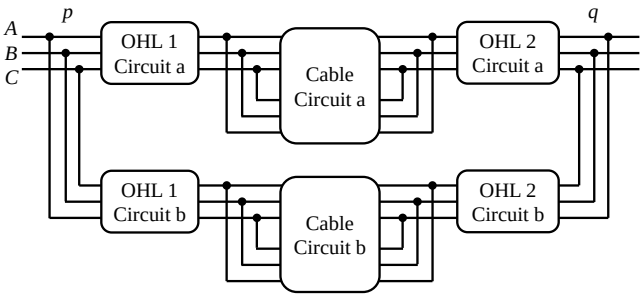


Fig. 1. General configuration of combined OHL and cable 380 kV transmission system.

### A. Configuration of Cable

There are in total 12 mutually coupled underground cables; the six parts of each actual cable can be represented by four equivalent parts: core conductor, insulation, earth screen, and outer sheath, see [3], [6], [7], and Fig. 2. The cable dimensions and properties are given in Table I.

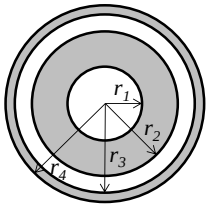


Fig. 2. Cable radii, $r_1$: core conductor, $r_1 - r_2$: insulation, $r_2 - r_3$: earth screen, $r_3 - r_4$: outer sheath.

The cable total length is 10.8 km, and is composed of 12 minor sections (MS01-MS12) with different length, earth resistivity, and trench type (see Fig. 3). Detailed information can be found in Table II. The supplied values are typical ones, but can have a slight variation in practice. In the reference model, 12 cable minor sections are assumed to have the same trench type, earth resistivity and length so that it is easier for studying the impact of changing each parameter.

TABLE I
Parameters for Cable Cross-sectional Model (Fig. 2)

| | Radius (mm) | Resistivity (Ωm) | Relative Permittivity |
|---|---|---|---|
| $r_1$ | 30.7 | $2.0\times10^{-8}$ | - |
| $r_2$ | 60.4 | - | 2.7 |
| $r_3$ | 62.8 | $7.3\times10^{-8}$ | - |
| $r_4$ | 67.9 | - | 2.3 |

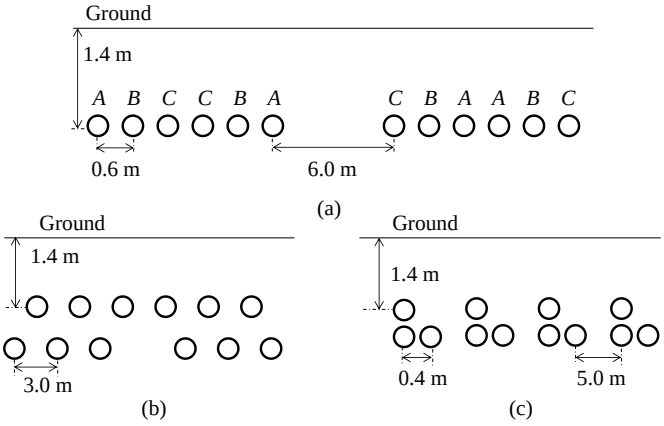


Fig. 3. Three trench types in applied cable system: open trench (a); horizontal directional drilling (HDD1, b), and (HDD2, c).

TABLE II
12 Minor section (MS), OHL1, and OHL2 Default Parameters

| | Trench type | Earth resistivity (Ωm) | Length (km) |
|---|---|---|---|
| MS 01-12 | Open trench | 100 | 0.9 |
| OHL1 | - | 100 | 4.0 |
| OHL2 | - | 100 | 6.0 |

All minor sections are connected successively via cable joints which directly connect the conductive core of cables and either cross-bond or terminate the screen layer. Three minor sections are grouped to one major section. Within each major section, two neighboring minor sections are connected via cable cross-bonding joints (see Fig. 4a). As proposed in [3] the impedance introduced by the cross-bonding is represented by a 1 μH inductance. Two major sections are connected via cable straight-through joint (see Fig. 4b) with impedance of 10 μH [3]. Surge arresters, to protect earth sheaths in cross-bonding joints from overvoltages are not modeled. For standard switching-surge waveform studied in this paper, no appreciable overvoltage on these sheaths occurs and the arrestors are considered as high impedances. Clearly, for steep fronts from lightning strikes or switching nearby the effect should be included.

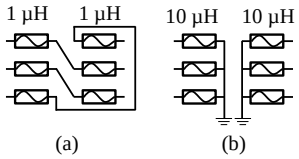


Fig. 4. Cable joints connecting the screen layers between two neighboring minor sections: cross-bonding joint (a); straight through joint (b).

### B. Configuration of OHL1 and OHL2

The tower for the part indicated with "OHL1" (in Fig. 1) is shown in Fig. 5-left. There is a double-circuit of 380 kV lines and a double-circuit of 150 kV lines, and two earth wires at the top of the towers. In the part indicated with "OHL2" the configuration is the similar as "OHL1", except for the 150 kV lines, see Fig. 5-right. The 380 kV lines are composed by a bundle of four sub-conductors. The parameters for the conductors in OHL are shown in Table III, where the bundle of four sub-conductors is already transferred to one equivalent conductor as described in [8].

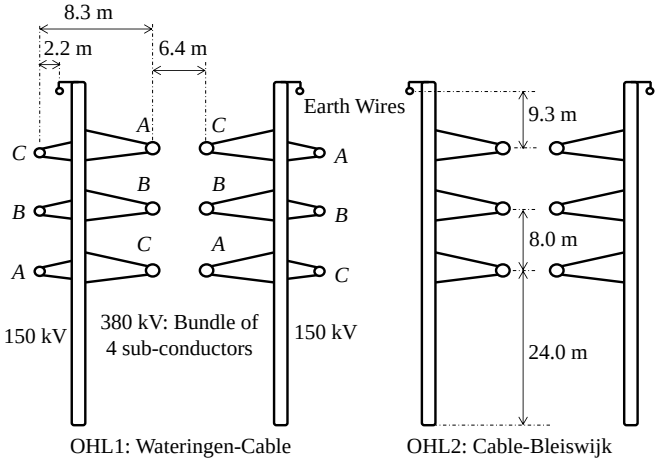


Fig. 5. Configuration of OHL1 and OHL2 pylons.

TABLE III
PARAMETERS USED FOR MODELING OHL1 AND OHL2 CONDUCTORS

| Lines | Radius (mm) | Resistivity (Ωm) |
|---|---|---|
| 380 kV | 231.3 | $2.1\times10^{-6}$ |
| 150 kV | 16.2 | $4.0\times10^{-8}$ |
| Earth wires | 10.9 | $4.8\times10^{-8}$ |

## III. TRANSIENT ANALYSIS IN FREQUENCY DOMAIN

Electromagnetic transients (response to a disturbance) can be efficiently analyzed in frequency domain using the so-called ABCD-matrix.

### A. ABCD-Matrix

Fig. 6 depicts a general transmission line representing any number of conductors.

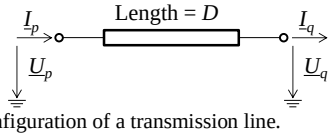


Fig. 6. General configuration of a transmission line.

The corresponding differential equations based on impedance **Z** and admittance **Y** matrices are:

$$-\frac{\mathrm{d}}{\mathrm{d}x}\mathbf{U}=\mathbf{Z}\cdot\mathbf{I},\qquad -\frac{\mathrm{d}}{\mathrm{d}x}\mathbf{I}=\mathbf{Y}\cdot\mathbf{U} \tag{1}$$

The formulas to establish **Z** and **Y** matrices for both cable and OHL can be found in [6], [7]. The ABCD-matrix is obtained as

$$\begin{bmatrix}\mathbf{U}_p\\ \mathbf{I}_p\end{bmatrix}=\begin{bmatrix}\mathbf{A} & \mathbf{B}\\ \mathbf{C} & \mathbf{D}\end{bmatrix}\begin{bmatrix}\mathbf{U}_q\\ \mathbf{I}_q\end{bmatrix}$$

where

$$\begin{bmatrix}\mathbf{A} & \mathbf{B}\\ \mathbf{C} & \mathbf{D}\end{bmatrix}=\left(\mathbf{T}\mathrm{e}^{\Lambda D}\mathbf{T}^{-1}\right)^{-1}$$

The columns of the matrix **T** collect the eigenvectors of the following matrix

$$\begin{bmatrix}\mathbf{O} & -\mathbf{Z}\\ -\mathbf{Y} & \mathbf{O}\end{bmatrix}$$

and the corresponding eigenvalues are located along the main-diagonal of matrix Λ, leaving all the off-diagonal elements zero. *D* is the length of the line.

According to the connection scheme shown in Fig. 1, the modeling method of parallel connection given in [4] is applied to generate the final ABCD-matrix for a three-phase system:

$$\begin{bmatrix}\underline{U}_{Ap}\\ \underline{U}_{Bp}\\ \underline{U}_{Cp}\\ \underline{I}_{Ap}\\ \underline{I}_{Bp}\\ \underline{I}_{Cp}\end{bmatrix}=\begin{bmatrix}\mathbf{A} & \mathbf{B}\\ \mathbf{C} & \mathbf{D}\end{bmatrix}\begin{bmatrix}\underline{U}_{Aq}\\ \underline{U}_{Bq}\\ \underline{U}_{Cq}\\ \underline{I}_{Aq}\\ \underline{I}_{Bq}\\ \underline{I}_{Cq}\end{bmatrix} \tag{2}$$

### B. Response to Disturbance

Resonant transients can be excited by disturbances like switching operation. Its effect is equivalent to adding a source at the switching moment [9]. Fig. 7 provides a scenario having a voltage-related disturbance (indicated by $u_S(t)$) at the *p* terminal of a three-phase transmission line with its *q* terminal open-ended.

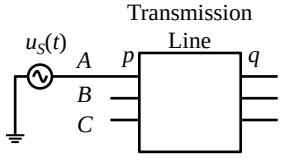


Fig. 7. Equivalent circuit diagram for analyzing of disturbance response.

Assume the aim is to obtain the time-domain response of the voltage at *q* terminal in phase *A*, $u_{Aq}(t)$. The transfer function describing the relationship between voltages at *q* and *p* terminals in phase *A* with various frequencies: $\underline{U}_{Aq}(\omega_k) = \underline{H}(\omega_k)\cdot\underline{U}_{Ap}(\omega_k)$ (with $k = 1,\ldots,n$), can be obtained by applying the open-ended condition (3) to (2).

$$\underline{I}_{Bp}=\underline{I}_{Cp}=\underline{I}_{Aq}=\underline{I}_{Bq}=\underline{I}_{Cq}=0 \tag{3}$$

$\underline{U}_{Ap}(\omega_k)$ is obtained by applying DFT to $u_{Ap}(t)$ which is equal to $u_S(t)$. Consequently, $u_{Aq}(t)$ can be calculated by transferring all $\underline{U}_{Aq}(\omega_k)$ to time-domain. The transfer function $\underline{H}$ serves as the fingerprint of a transmission line providing all information of each particular configuration for the response upon a disturbance and forms the basis for comparison and analysis of varied parameters of the transmission line shown in Fig. 1.

## IV. Analysis for Different Configurations

The standard switching surge (250/2500 μs) is adopted to serve as an example, see Fig. 8. Based on the reference configuration described in Section II, the impact of parameter variation upon switching surge under no-load operation is analyzed:

Fig. 9: different area of the conductive core of each cable;
Fig. 10: different earth resistivity;
Fig. 11: different trench types;
Fig. 12: different phase sequence;
Fig. 13: different length of each cable minor section;
Fig. 14: different total length of cable (number of major sections);
Fig. 15: different number of cables;
Fig. 16: with and without cable;
Fig. 17: with and without cable joints;
Fig. 18: different combinations of cable and OHL.

The time domain responses (top figures in Fig. 9 to Fig. 18) are a combination of the input voltage in frequency domain (Fig. 8-bottom) and the transfer function of each particular scenario (bottom figures in Fig. 9 to Fig. 18). A global explanation is presented below.

Fig. 9 shows that by increasing the conductive core radius of each cable, the first resonant frequency in the transfer function is lowered since the cable capacitance is increased (about 0.1 μF/km for 50% of $r_1$, 0.2 μF/km for $r_1$, and 0.4 μF/km for 200% of $r_1$, calculated by PSCAD/EMTDC), and the waveforms in Fig. 9-top shift accordingly. Fig. 10 indicates that earth composed by loam clay; swamp marl or humid sand will have virtually the same resonant transient behavior. The values of earth resistivity of different earth types are given in [10]. Although there are differences in the transfer functions (from 2 kHz to 6 kHz) shown in Fig. 11 (different trench types) and Fig. 12 (different phase sequence), their responses to the switching surge are similar, since in that frequency range the input voltage in frequency domain is small. One of the main cable properties affecting resonance is its capacitance. With shorter length of each minor section (Fig. 13), fewer major sections (Fig. 14), lower number of cables (Fig. 15), and especially in absence of the cable at all (Fig. 16), the capacitance of the transmission line is reduced. Therefore, the resonant frequency increases. This can be verified by the bottom graphs in Fig. 13-16. Besides, although Fig. 15-bottom shows that by reducing the number of cables from 12 to 6 the magnitude of the first peak in transfer function is increased from about 16 to 20, Fig. 15-top presents similar magnitude of the resonance in time-domain. The reason is that the first peaks in the transfer functions occur around 1 kHz, but around this frequency, the magnitude of the input voltage in frequency domain decreases with frequency (Fig. 8-bottom). Removing the cable joints eliminates all resonances between 3 kHz to 6 kHz (Fig. 17-bottom), and changing the combination of OHL and cable from OHL1-Cable-OHL2 to OHL1-OHL2-Cable shifts the first resonance to a lower frequency in the transfer function (Fig. 18-bottom). In all frequency responses shown in Fig. 9 to Fig. 18, the transfer function always equals 1 at DC, due to the fact that the transmission line has no capacitive or inductive behavior at DC.

The adopted approach is compared with PSCAD results based on a simplified cable configuration, which can be implemented in PSCAD. The mutual coupling of the two cable circuits is ignored. The result is depicted in Fig. 19, which confirms that both approaches give virtually equal results. The adopted method (implemented as MATLAB code without optimizing for calculation speed [11]) for the specific calculations for Fig. 19 was over a factor of 50 faster than PSCAD/EMTDC software using the same platform. It must be noted that gain in computation speed depends on the topology to be analyzed.

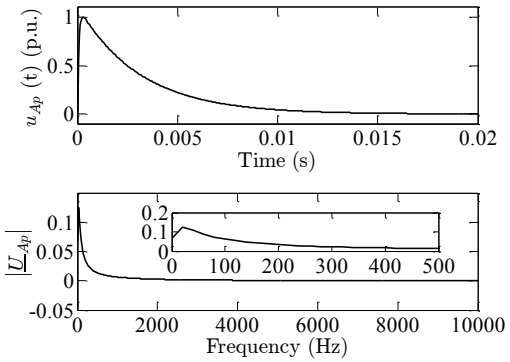


Fig. 8. Input voltage: top – time domain; bottom – frequency domain

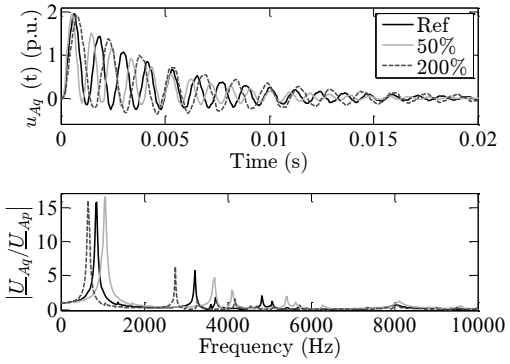


Fig. 9. Comparison with different conductive core radius ($r_1$) for three cases: 30.7 mm (Ref), 50%·Ref, and 200%·Ref.

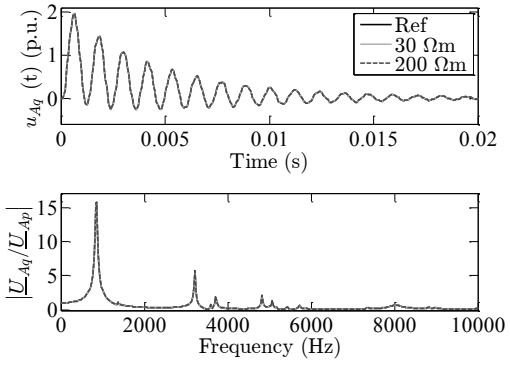


Fig. 10. Comparison with different earth resistivity for three cases: 100 Ωm for loam clay (Ref), 30 Ωm for swamp marl, and 200 Ωm for humid sand.

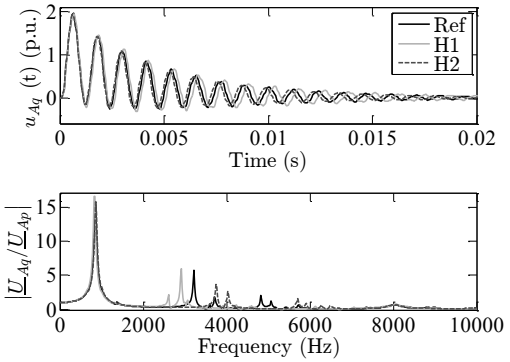


Fig. 11. Comparison with different trench types for three cases: open trench (Ref), HDD1 (H1), and HDD2 (H2).

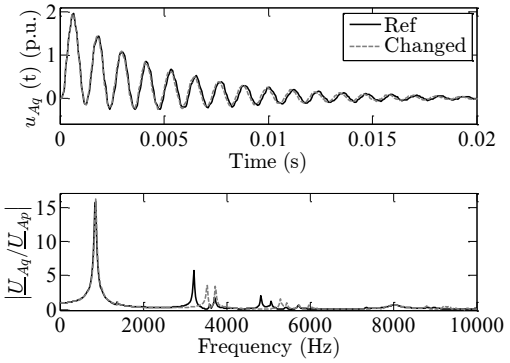


Fig. 12. Comparison with different phase sequences for two cases: ABC-CBA-CBA-ABC (Ref) and ABC-ABC-CBA-CBA (Changed).

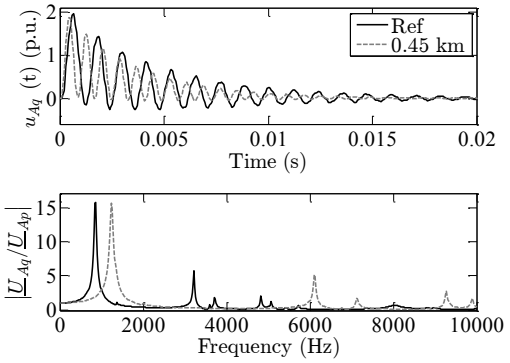


Fig. 13. Comparison with different lengths of minor section for two cases: 0.9 km (Ref) and 0.45 km. The number of minor section is kept as 12.

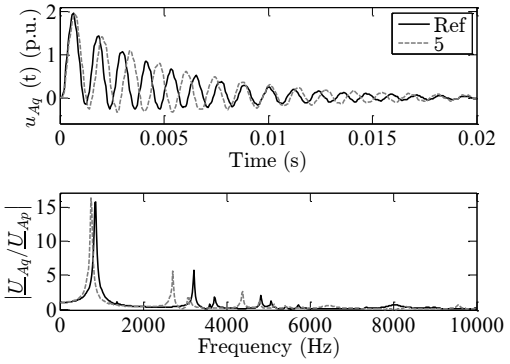


Fig. 14. Comparison with different number of major sections for two cases: 4 (Ref) and 5. The length of minor section is kept as 0.9 km.

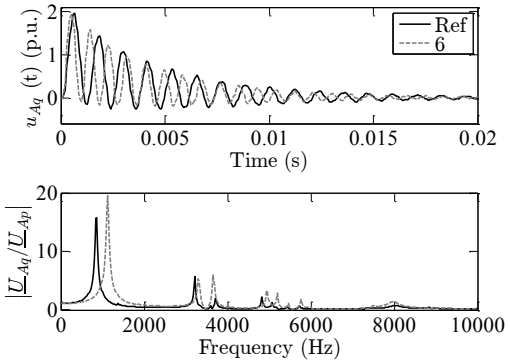


Fig. 15. Comparison with different cable number for two cases: 12 cables (Ref) and 6 cables (each circuit has only one cable per phase). The distance between two cable circuits is kept as 6 m.

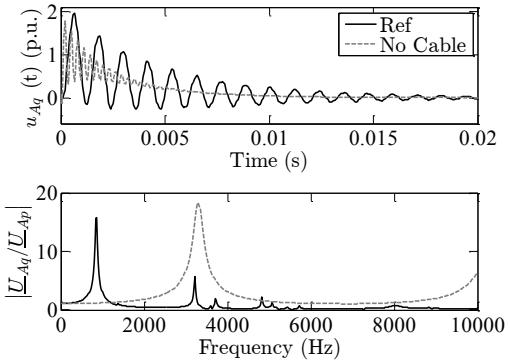


Fig. 16. Investigation of the impact of cable: OHL1-Cable-OHL2 (Ref) and OHL1-OHL2, where the cable is replaced by extending of OHL2 (4 km of OHL1 and 16.8 km of OHL2).

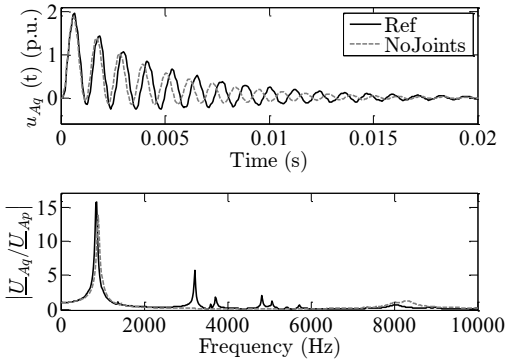


Fig. 17. Investigation of the impact of cable joints: Ref means with joints.

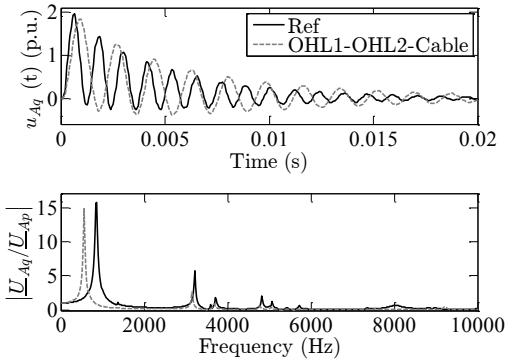


Fig. 18. Comparison with different combination of OHL and cable for two cases: OHL1-Cable-OHL2 (Ref) and OHL1-OHL2-Cable.

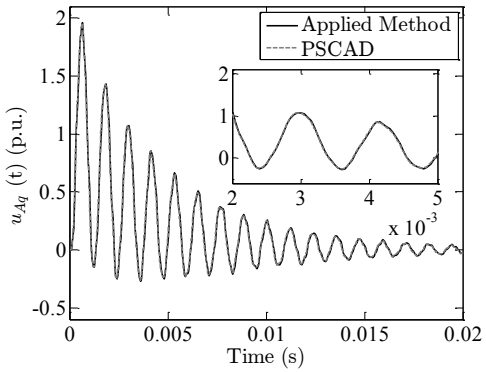


Fig. 19. Comparison of the applied method (transient analysis in frequency domain) with PSCAD/EMTDC (simulation in time-domain based on EMTP-theory) when the mutual coupling between two cable circuits is ignored.

## V. Conclusions

This paper describes the approach of frequency domain transient analysis for a complex transmission line (composed by mixed OHL and cable), and also investigated the impact of changing network configurations on the switching surge response in no-load condition. These studies are difficult to be effectively realized by EMTP-theory based simulation tools. Since both methods adopts the same general formulation of impedance and admittance matrices the results should be equal, which was confirmed.

The application of this approach on investigating different network configurations shows that with increased conductive core radius of each cable, cable length, cable number, and with placing the cable to the right-hand-side will have a lower resonant frequency of the first peak in the corresponding transfer function plot. The application of cable joints causes more high frequency components. With the considered parameter values, the influence of earth resistivity, trench types, and phase sequence can be ignored.

Another advantage of the frequency domain analysis shown in this paper is that it can provide specific information for understanding the transient behavior, since each frequency point can be evaluated and analyzed individually, while in time domain simulation, the time-domain voltages and currents have to depend on their historical values gradually accumulated by simulation time steps [5], [6].

## VI. References

[1] M. Rebolini, L. Colla, and F. Iliceto. "400 kV AC new submarine cable links between Sicily and the Italian mainland. Outline of project and special electrical studies," In *CIGRE Session*, vol. 2008, pp. C4-116. 2008.

[2] W. L. Weeks, Y. M. Diao, "Wave Propagation Characteristics In Underground Power Cable," *IEEE Trans. Power Apparatus and System*, vol.PAS-103, no.10, pp. 2816-2826, Oct. 1984.

[3] U.S. Gudmundsdottir, B. Gustavsen, C. L. Bak, and W. Wiechowski. "Field test and simulation of a 400-kV cross-bonded cable system," *IEEE Trans. Power Delivery*, 26(3):1403 –1410, July 2011.

[4] L. Wu, P. A. A. F. Wouters, and E. F. Steennis. "Model of a double circuit with parallel cables for each phase in a HV cable connection," *Power System Technology (POWERCON), 2012 IEEE International Conference on*, vol., no., pp.1-5, Oct. 30 2012-Nov. 2 2012.

[5] H. W. Dommel. *Electromagnetic Transients Program: Reference Manual: (EMTP theory book)*. Bonneville Power Administration, 1986.

[6] Manitoba HVDC Research Centre Inc. *EMTDC User's Guide*, volume 4.7, fifth printing. February 2010.

[7] A. Ametani. "A general formulation of impedance and admittance of cables," *IEEE Trans. Power Apparatus and Systems*, (3):902– 910, 1980.

[8] W.D. Stevenson and J.J. Grainger. *Power System Analysis*. Nova Iorque: McGraw-Hill International Editions, 1994, pp. 141-190.

[9] A. Greenwood. *Electrical Transients in Power Systems*, John Wiley & Sons, INC., Second Edition, 1991, pp. 6-9.

[10] P. Denzel, *Grundlagen der Übertragung elektrischer Energie.* Springer, 1966, p. 289.

[11] D. J. Higham, N. J. Higham, *MATLAB guide*, Society for Industrial and Applied Mathematics, 2005, pp. 297-305.